

Received May 30, 2013; reviewed; accepted, July 23, 2013

SYNTHESIS AND PHYSICOCHEMICAL CHARACTERISTICS OF TITANIUM DIOXIDE DOPED WITH SELECTED METALS

**Katarzyna SIWINSKA-STEFANSKA^{*}, Dominik PAUKSZTA^{*},
Adam PIASECKI^{**}, Teofil JESIONOWSKI^{*}**

^{*} Poznan University of Technology, Faculty of Chemical Technology, Institute of Chemical Technology and Engineering, Marii Skłodowskiej-Curie 2, PL-60-965, Poznan, Poland; e-mail: Katarzyna.Siwinska-Stefanska@put.poznan.pl, phone: +48 616653626, fax: +48 616653649

^{**} Poznan University of Technology, Faculty of Mechanical Engineering and Management, Institute of Materials Science and Engineering, Jana Pawla II 24, PL-60-965, Poznan, Poland

Abstract: The paper details with of the preparation and physicochemical characterisation of nano- and microstructured TiO₂ doped with Fe and Co produced by the sol-gel method using titanium alkoxide as the precursor of titania as well as iron or cobalt nitrates as dopant sources. Fe and Co doped TiO₂ materials were successfully prepared with two different methods. The effect of the dopant type on the synthesis of TiO₂ powders was investigated. The physicochemical properties of the studied samples were determined. The characterisation included determination of the dispersion and morphology of the systems (particle size distribution, SEM images), characteristics of porous structure (BET isotherms), crystalline structure (XRD), surface composition (EDS), as well as thermal stability (TG/DTA).

Keywords: titanium dioxide, sol-gel method, doping, TiO₂ surface modification, Fe and Co dopant

Introduction

Titanium dioxide (TiO₂) has emerged as one of the most fascinating materials in the modern era. It has captured the attention of physical chemists, physicists, material scientists, and engineers exploring distinctive semiconducting and photocatalytic properties (Wu, 2007; Huang, 2009; Wang, 2009; Xu, 2011; He, 2012). Inertness to the chemical environment and long-term photostability has made TiO₂ an important component in many practical applications and in commercial products. From drugs to doughnuts, cosmetics to catalysts, pigments to pharmaceuticals, and sunscreens to solar cells, TiO₂ is used as a desiccant, brightener, or reactive mediator.

Titanium dioxide represents an effective photocatalyst for water and air purification and for self-cleaning surfaces. Additionally, it can be used as an antibacterial agent because of strong oxidation activity and superhydrophilicity (Fujishima, 2006). TiO_2 shows relatively high reactivity and chemical stability under ultraviolet light ($\lambda < 387 \text{ nm}$), whose energy exceeds the band gap of 3.3 eV in the anatase crystalline phase. The development of photocatalysts exhibiting high reactivity under visible light ($\lambda > 400 \text{ nm}$) should allow the main part of the solar spectrum to be used, even under poor illumination of interior lighting. Several approaches to modifying TiO_2 have been proposed: metal-ion implanted TiO_2 (using transition metals: Cu, Co, Ni, Cr, Mn, Mo, Nb, V, Fe, Ru, Au, Ag, Pt) (Anpo, 2000; Fuente, 2001; Yamashita, 2001), reduced TiO_x photocatalysts (Takeuchi, 2000; Ihara, 2001), non-metal doped- TiO_2 (N, S, C, B, P, I, F) (Ohno, 2003; Yu, 2003; Liu, 2005), composites of TiO_2 with semiconductor having lower band gap energy (e.g., Cd-S particles (Hirai, 2001), sensitizing of TiO_2 with dyes (e.g., thionine) (Chatterjee, 2001) and TiO_2 doped with upconversion luminescence agent (Zhou, 2006; Wang, 2007).

The aim of the study was verification of preparation methods of TiO_2 doped with metallic species, including two types of dopants and doping methods. The effect of the doping process on the fundamental physicochemical properties for all obtained samples was evaluated.

Experimental

Materials

The pure and doped TiO_2 powders were synthesized employing the sol-gel method, in which titanium tetraisopropoxide ($\text{Ti}(\text{OC}_3\text{H}_7)_4$, 97%) was used as the precursor of titania, ammonia (NH_4OH , 25%) as catalyst, 2-propanol ($\text{C}_3\text{H}_7\text{OH}$, 99.5%) as solvent, iron(III) nitrate ($\text{Fe}(\text{NO}_3)_3 \cdot 9\text{H}_2\text{O}$, 98%) and cobalt(II) nitrate ($\text{Co}(\text{NO}_3)_2 \cdot 6\text{H}_2\text{O}$, 98%) as dopant sources.

Synthesis of TiO_2 via sol-gel method

TiO_2 powder was prepared by a sol-gel process, in which sol was prepared by mixing titanium tetraisopropoxide (TTIP), 2-propanol, and ammonia at room temperature. 15 cm^3 (0.049 mole) of TTIP as the starting material was dissolved in 100 cm^3 (1.304 mole) of 2-propanol. Upon stirring the catalyst, ammonia was introduced at a constant rate of 1 cm^3/min . The titanium alkoxide solution was hydrolysed by adding 15 cm^3 (0.033 mole) of ammonia. The initially clear solution turned into a white emulsion. This solution was vigorously stirred for 1 h. The entire system was transferred to a round-bottomed flask and placed in a vacuum rotary evaporator, in order to remove the solvent (water bath temperature 60 °C, pressure 136 mbar). The subsequent stage involved filtration of the mixture under reduced pressure. The sample obtained in this way was washed with distilled water. At the terminal stage, the sample was dried by

convection at 105 °C for 18 h. The sample was then calcined at 600 °C for 2 h. The proposed method for preparing TiO₂ is presented schematically in Fig. 1a.

Synthesis of doped-TiO₂

The doped-TiO₂ materials were prepared following two different methods. The first method: solution A was prepared by adding 15 cm³ (0.049 mole) of titanium tetraisopropoxide to 100 cm³ (1.304 mole) of 2-propanol. A certain amount of Fe(NO₃)₃ or Co(NO₃)₂ was dissolved in 100 cm³ (0.782 mole) of 2-propanol (solution B). Subsequently, solution B and ammonia (catalyst – solution C) were introduced to solution A, at a constant rate of 5 and 1 cm³/min, respectively. The resulting solution was vigorously stirred. When dosing of solutions B and C was terminated, the emulsion obtained was mixed for 30 min. The second method: solution A was prepared by adding 15 cm³ (0.049 mole) of titanium tetraisopropoxide to 50 cm³ (0.670 mole) of 2-propanol. At first, a certain amount of Fe(NO₃)₃ or Co(NO₃)₂ was dissolved in 100 cm³ (0.782 mole) of 2-propanol and then the solution obtained (solution B) was dosed to solution A at a constant rate of 5 cm³/min. The obtained solution was vigorously stirred. Next, 15 cm³ (0.033 mole) of ammonia was dissolved in 50 cm³ (0.670 mole) of 2-propanol (solution C) and then the resulting mixture was introduced to a mixture of solution A and B, at a constant rate of 1 cm³/min. When dosing of solution C was terminated, the obtained emulsion was mixed for 30 min. The concentrations of Fe and Co calculated for mass of the dry sample of titania were 0.10; 0.25; 0.57; 0.75; 1.00; 1.70 and 2.80% mass, respectively. Classification of the obtained products was realised in analogous way as in the case of preparation titanium dioxide. The final products of Fe- and Co-doped titania have a yellow/orange and green colour, respectively. Fig. 1 b and c presents two doping methods of titania.

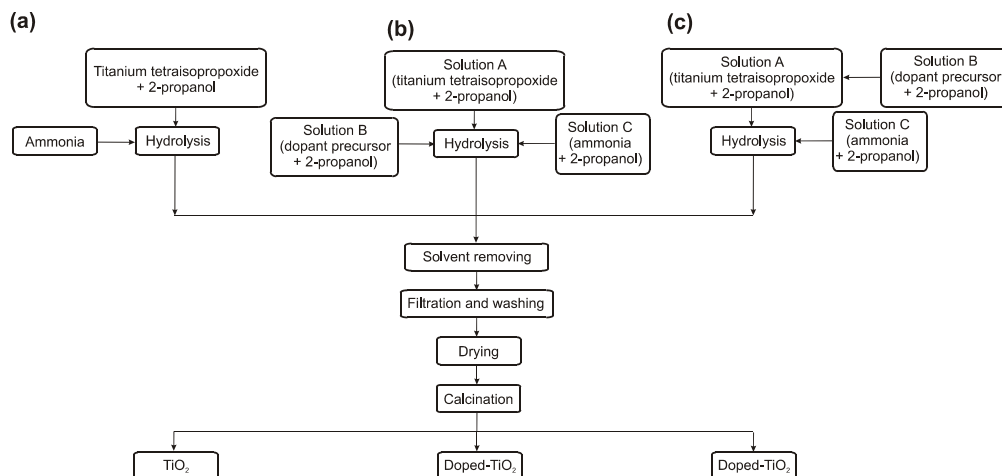


Fig. 1. Preparation of (a) TiO₂ and doped-TiO₂ by (b) first method, (c) second method via sol-gel method

Determination of physicochemical properties

The doped-TiO₂ samples were subjected to comprehensive characterisation using the most advanced analytical methods and techniques. The dispersive properties of TiO₂/Fe and TiO₂/Co samples were evaluated based on the particle size distributions and polydispersity index (PDI) determined using a Zetasizer Nano ZS made by Malvern Instruments Ltd. operating based on non-invasive back scatter technique. The samples of doped-TiO₂ were also subjected to morphological and microstructural analysis using a scanning electron microscope – Zeiss EVO40. In order to characterise their porous structure, nitrogen adsorption/desorption isotherms at 77 K and parameters such as surface area (A_{BET}), pore volume (V_p) and average pore size (S_p) were determined using an ASAP 2020 instrument (Micromeritics Instrument Co.). All samples were degassed at 120 °C for 4 h prior to measurement. The surface area was determined by the multipoint BET (Brunauer–Emmett–Teller) method using the adsorption data in the relative pressure (p/p_0). The BJH (Barrett–Joyner–Halenda) method was applied to determine the pore volume and the average pore size. The doped-TiO₂ samples were also subjected to crystalline structure determination using the WAXS method (wide-angle X-ray scattering). X-ray diffraction measurements were performed using Cu K α ($\lambda=1.54056$ Å) radiation. The accelerating voltage and the applied current were 30 kV and 15 mA respectively. The samples were scanned at a rate of 0.04° over an angular range of 5–60°. Moreover, the surface composition of the obtained materials was analysed using an EDS technique (energy dispersive X-ray spectroscopy) using a Princeton Gamma-Tech unit equipped with a prism digital spectrometer. Thermogravimetric analysis was performed using a Jupiter STA 449 F3 (Netzsch GmbH). Samples weighing approximately 10.0 mg were placed in an Al₂O₃ crucible, and heated at a rate of 10 °C/min from 30 to 1000 °C in a nitrogen atmosphere.

Results and discussion

The aim of the first stage of the study was to characterise the dispersive properties and morphology of the pure TiO₂ obtained via the sol-gel method. The titanium dioxide is characterised by a monomodal particle size distribution with a relatively wide band covering the diameter range of 955–2670 nm. The maximum volume contribution of 28.4% corresponds to agglomerates of 1720 nm in diameter (Fig. 2a). The polydispersity index of TiO₂ is 0.153, which means that this sample is rather homogeneous. The SEM microphotograph of the titanium dioxide studied presented in Fig. 2b confirms the presence of particles of micro-sized diameter (corresponding to those indicated in the particle size distribution), their almost spherical shape and high homogeneity.

The structure of obtained sample was studied using the WAXS method. The crystalline structure of sample determines their suitability for particular applications (catalysis, paints, lacquers, and polymer fillers). Titania of well-defined crystalline

structure shows diffraction maxima at certain specific 2-theta values. Figure 2c shows the WAXS pattern of prepared TiO₂ sample of the anatase structure, characterised by the presence of maxima at 2Θ values of 25, 38, 48, 54 and 55, which is a confirmation of the effective preparation process (JCPDS, Card 21-1272.).

Characterisation of the porous structure of pure TiO₂ included determination of the nitrogen adsorption/desorption isotherms and calculation of the surface area, size and volume of pores. Synthetic TiO₂, obtained via the sol-gel method, has defined surface activity, which is indicated by its specific surface area of 17.4 m²/g. It can be classified as mesoporous adsorbent as its pore volume is $V_p = 0.013 \text{ cm}^3/\text{g}$ and pore diameter is $S_p = 2.9 \text{ nm}$.

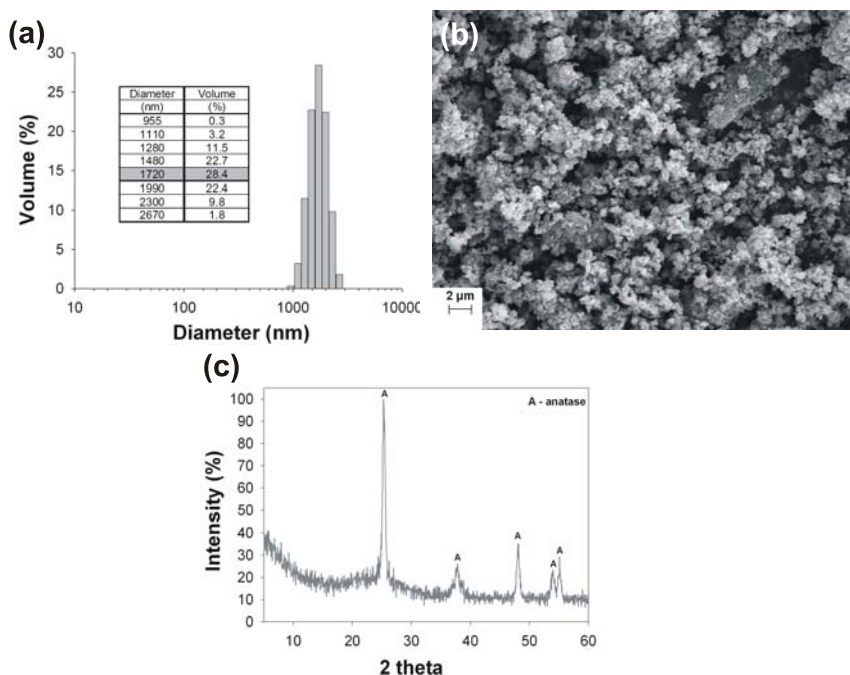


Fig. 2. Particle size distribution (a), SEM microphotograph (b) and WAXS pattern (c) of TiO₂ obtained via sol-gel method

At the next stage, the titanium dioxide preparation process was supplemented with doping using selected metals (Fe and Co). The main aim of the study was to evaluate the efficiency of the doping process of synthetic titanium dioxide and to determine its influence on the fundamental physicochemical properties of the obtained systems. Samples of TiO₂ doped with Fe and Co were subjected to dispersive and morphological characterisation. Table 1 presents the dispersive characteristics of doped-TiO₂ samples. The results prove that the doping process caused significant changes in the dispersive character of the obtained systems.

Table 1. Dispersive properties of doped-TiO₂ obtained via sol-gel method

Amount of metal dopant (% mass)	Particle size distributions by volume (nm) and maximum volume contribution (%)	Polydispersity index
TiO ₂ /Fe (first method)		
0.10	295–1110 (531 nm – 24.9)	0.329
0.57	255–825 (459 nm – 25.5)	0.191
1.00	220–615 (396 nm – 27.3)	0.298
2.80	190–825 (396 nm – 8.7) 3090–6440 (5560 nm – 25.7)	0.424
TiO ₂ /Fe (second method)		
0.10	342–955 (615 nm – 29.2)	0.079
0.57	342–1280 (712 nm – 23.4)	0.342
1.00	531–1990 (1280 nm – 20.2)	0.099
2.80	396–1480 (712 nm – 23.7)	0.264
TiO ₂ /Co (first method)		
0.10	531–1480 (955 nm – 26.3)	0.098
0.57	615–1720 (1110 nm – 25.3)	0.247
1.00	255–615 (459 nm – 28.6)	0.417
2.80	295–825 (531 nm – 27.7)	0.205
TiO ₂ /Co (second method)		
0.10	531–2300 (1280 nm – 19.7)	0.267
0.57	459–1720 (955 nm – 23.4)	0.305
1.00	531–1990 (1110 nm – 22.4)	0.195
2.80	342–1280 (615 nm – 22.8)	0.260

The substantial differences in the mean diameters of TiO₂ particles doped with two different metals in different amounts, imply that the dopant type have a great effect on the dispersive parameters of the final products. The dispersive characteristics show that noticeable changes in the particle size of all doped TiO₂ appear independently of the type and quantity of the dopant as well as the doping method. According to the results, by far the best dispersive properties are shown by materials doped with iron. All samples of the doped materials have particles of smaller diameter than those determined in the sample of pure titanium dioxide. In most samples, the doping of pure TiO₂ with selected dopant (in relation to the amount of dopant used) contributed to a decrease in the sample's homogeneity (higher polydispersity index) – see Table 1 – compared to that of pure titania.

The SEM microphotographs of the samples studied presented in Fig. 3 confirm the presence of particles of micro-sized diameter (corresponding to those indicated in particle size distributions), high homogeneity, almost spherical shape and showing a small tendency to form agglomerate structures.

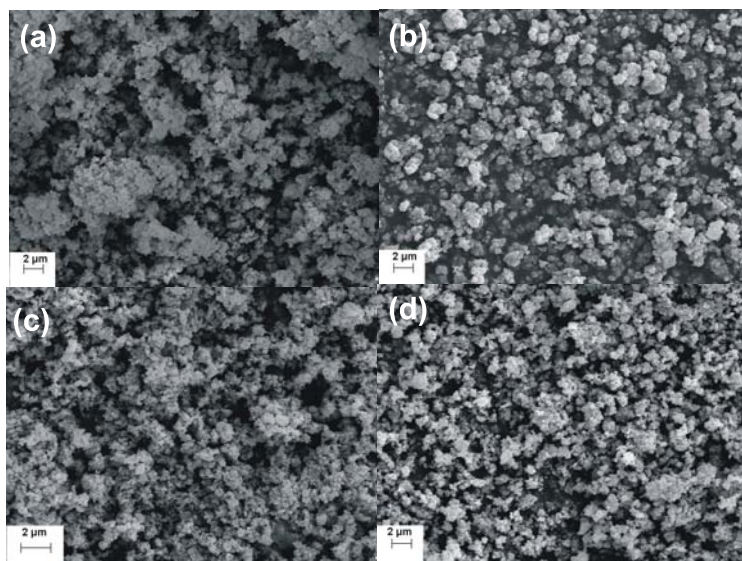


Fig. 3. SEM microphotographs of TiO₂ doped with 1.0% mass of Fe (first method – a), 1.0% mass of Fe (second method – b), 1.0% mass of Co (first method – c) and 1.0% mass of Co (second method – d)

The XRD patterns of different TiO₂ samples (pure, Fe and Co doped) are shown in Fig. 4. The XRD pattern of pure TiO₂ shows five primary peaks at 25, 38, 48, 54 and 55, which can be attributed to different diffraction planes of anatase. The XRD patterns of doped samples show different peaks at 28, 36, 39, 41, 44, 54 and 57, which resulted from different diffraction planes of the rutile form of TiO₂. Results show that the addition of iron or cobalt to the titania preparation process has a significant effect on crystalline structure formation. The XRD patterns of Fe and Co doped TiO₂ samples almost coincide with that of pure TiO₂, showing no diffraction peaks related

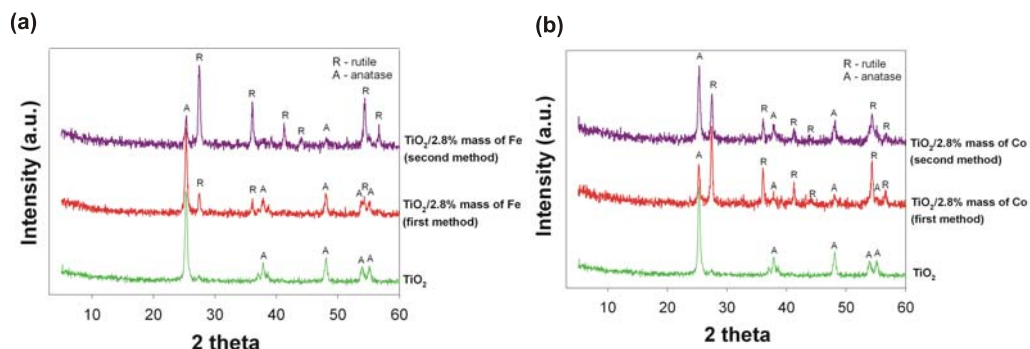


Fig. 4. WAXS patterns of TiO₂ doped with Fe (a) and Co (b)

with iron and cobalt. Our observations are in agreement with previous research (Amadelli, 2008; Ambrus, 2008; Hamadani, 2010). It can be concluded that selected dopants are not incorporated directly onto titania structure, but are placed onto the TiO_2 surface. Fe^{3+} and Co^{2+} ions influence the crystalline structure formation of TiO_2 and cause the transformation of the anatase phase to rutile.

At the next stage of the study, the adsorption abilities of the doped titanium dioxide samples were characterised. The fundamental parameters determining the surface activity of the doped samples, the surface area (BET) and pore size distribution, are given in Table 2.

Table 2. Porous structure parameters of native and doped- TiO_2

Amount of metal dopant (% mass)	A_{BET} (m^2/g)	V_p (cm^3/g)	S_p (nm)	A_{BET} (m^2/g)	V_p (cm^3/g)	S_p (nm)
	TiO_2/Fe (first method)			TiO_2/Co (first method)		
0.10	10.2	0.009	3.1	9.9	0.008	3.0
0.57	8.7	0.006	2.9	8.4	0.006	2.6
1.00	6.7	0.005	2.8	6.9	0.004	2.5
2.80	4.5	0.003	2.8	4.3	0.004	2.5
	TiO_2/Fe (second method)			TiO_2/Co (second method)		
0.10	12.8	0.012	3.2	14.5	0.013	3.3
0.57	6.2	0.004	2.8	13.6	0.009	2.7
1.00	5.8	0.004	2.8	9.8	0.008	2.6
2.80	4.7	0.003	2.8	7.3	0.007	2.6

A considerable decrease in the surface area relative to that of the pure sample was observed for all doped samples. Addition of any of dopants also resulted in a decrease in the pore diameters relative to those of native TiO_2 , irrespective of the quantity of dopant. The BET surface areas decrease was observed together with increasing Fe and Co amount in the sample structure. The TiO_2 doped with Co obtained via first method has the lowest BET surface area as compared to Co doped TiO_2 obtained according to second method.

The surface composition of the obtained samples was studied by the EDS technique. EDS results are given in Table 3. From the elemental mapping mode, highly and uniformly dispersed Fe and Co on the TiO_2 support were observed. This implies good interaction between dopant and support in the preparation process using the sol-gel method. The EDS technique was used to detect the amount of Fe and Co in the titania structure. Doped titania samples contain ca. 0.12 and ca. 0.56% mass of Fe were produced via first method using 0.10 and 0.57% mass of Fe as a dopant. It can be seen that Fe amount is very close to the initial values. Wen et al. (2012) have observed

the analogous results. The EDS analysis of Fe and Co doped TiO₂ confirmed the presence of Fe and Co ions in the powder structure, as the opposite of XRD patterns. The XRD patterns do not show any peaks related to Fe and Co, presence in TiO₂ structure.

Table 3. Surface composition of doped-TiO₂

Amount of metal dopant (% mass)	Compound content (%)					
	Ti	O	Fe	Ti	O	Co
	TiO ₂ /Fe (first method)			TiO ₂ /Co (first method)		
0.10	54.92	44.95	0.12	52.10	47.85	0.05
0.57	51.08	48.36	0.56	55.44	44.13	0.43
1.00	50.06	49.12	0.82	51.63	47.74	0.63
2.80	54.13	43.82	2.05	55.86	42.18	1.96
	TiO ₂ /Fe (second method)			TiO ₂ /Co (second method)		
	Ti	O	Fe	Ti	O	Co
0.10	50.61	49.19	0.20	50.11	49.83	0.06
0.57	48.77	50.62	0.61	50.80	48.78	0.42
1.00	52.32	46.79	0.89	52.01	47.41	0.58
2.80	51.07	46.83	2.10	51.13	47.08	1.79

Investigation of the effectiveness of the doped process has been broadened by thermal analysis TG/DTA (Fig. 5) of the pure TiO₂, and selected doped materials. The results of TG/DTA analysis allowed for an estimate of the temperature range that corresponds to important chemical and structural transitions of the obtained systems.

Figure 5a shows TGA thermograms of pure titanium dioxide and systems obtained by doping titania with 2.8% mass of Fe. Analysis of the obtained systems was performed in order to determine thermal stability. In case of pure titania, first mass loss is observable in a temperature range of 30 to 300 °C, and most likely corresponds to loss of physically and chemically bound water. At this point mass loss is slightly above 0.4%. Total mass loss of pure TiO₂ is equal to ~0.9%. The TGA thermograms of doped-TiO₂ with iron show similar changes in thermal stability in comparison to pure titania. Total mass loss of doped samples via first and second method is equal to ~0.7 and ~1.2%, respectively. A similar change of thermal stability was observed of Co-doped TiO₂ (Fig. 5b). Total mass loss of Co-doped samples via the first and second method is equal to ~0.75 and ~0.8%, respectively.

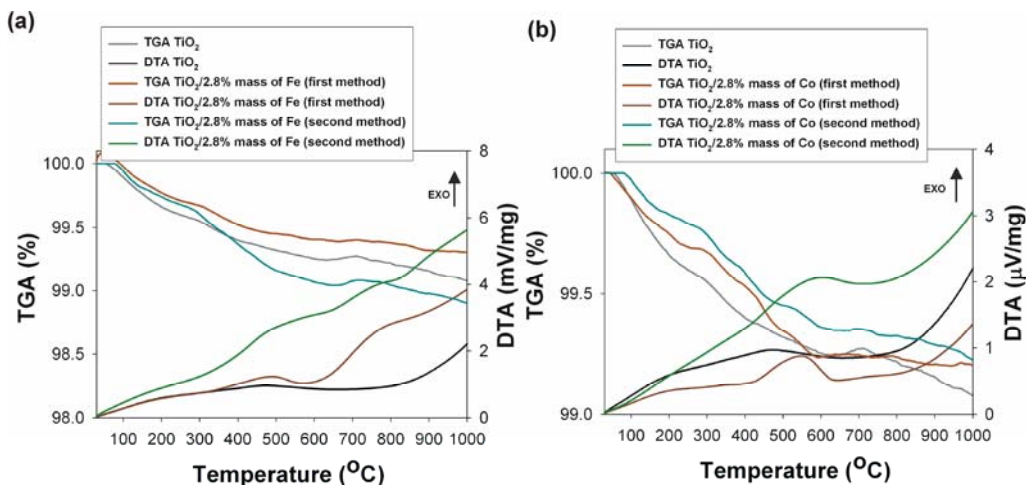


Fig. 5. Thermograms of doped TiO_2 with Fe (a) and Co (b) obtained by sol-gel method

Conclusions

According to the results presented above, the systems obtained after doping of selected dopants (Fe and Co) on titania were characterised by particles of smaller diameter and lower homogeneity compare to pure TiO_2 .

The XRD patterns show that the addition of iron or cobalt to the titania preparation process has a significant effect on crystalline structure formation. The XRD patterns of Fe and Co doped TiO_2 samples almost coincide with that of pure TiO_2 , showing no diffraction peaks related with iron and cobalt.

The type of dopant and doping method has a significant influence on the surface activity of the systems obtained by sol-gel method. The porous structure of the doped titania decreased proportionally with increasing concentration of the dopant. Surface area measurements were carried out on TiO_2 samples doped with Fe and Co, indicating that the adopted doping procedure brought some surface area change with respect to the pristine oxide.

Iron and cobalt were found to be effectively doped on the surface of synthetic the TiO_2 sample. EDS analysis of Fe and Co doped TiO_2 confirmed the presence of Fe and Co ions in the powder structure,

The Fe and Co doped titania acquired via doping of selected dopants are characterised by a small shift in thermal stability. However, a small change in the mass loss of doped samples, in comparison to pure titania, was observed.

Acknowledgements

This work was supported by Polish National Centre of Science research grant no. 2011/01/B/ST8/03961.

References

- AMADELLI R., SAMIOLO L., MALDOTTI A., MOLINARI A., VALIGI M., GAZZOLI D., 2008, *Preparation, characterisation, and photocatalytic behaviour of Co-TiO₂ with visible light response*, International Journal of Photoenergy, Article ID 853753, 9 pages, doi: 10.1155/2008/853753.
- AMBRUS Z., BALÁZS N., ALAPI T., WITTMANN G., SIPOS P., DOMBI A., MOGYORÓSI K., 2008, *Synthesis, structure and photocatalytic properties of Fe(III)-doped TiO₂ prepared from TiCl₃*, Applied Catalysis B: Environmental 81, 27–37.
- ANPO M., 2000, *Use of visible light. Second-generation titanium dioxide photocatalysts prepared by the application of an advanced metal ion-implantation method*, Pure and Applied Chemistry 72, 1787–1792.
- CHATTERJEE D., MAHATA A., 2001, *Demineralization of organic pollutants on the dye modified TiO₂ semiconductor particulate system using visible light*, Applied Catalysis B: Environmental 33, 119–125.
- FUERTE M.D.H.A., MAIRA A.J., MARTINEZ-ARIAS A., FERNADEZ-GARCIA M., CONESA J.C., SORIA J., 2001, *Visible light-activated nanosized doped-TiO₂ photocatalysts*, Chemical Communications 24, 2718–2719.
- FUJISHIMA X., ZHANG C.R., 2006, *Titanium dioxide photocatalysis: Present situation and future approaches*, Chimie 9, 750–760.
- HAMADANIAN M., REISI-VANANI A., MAJEDI A., 2010, *Sol-gel preparation and characterization of Co/TiO₂ nanoparticles: application to degradation of Methyl Orange*, Journal of the Iranian Chemical Society 7, S52–S58.
- HE Z.L., QUE W.X., XIE H.X., CHEN J., YUAN, P. SUN., 2012, *Facile synthesis of self-sensitized TiO₂ photocatalysts and their higher photocatalytic activity*, Journal of the American Ceramic Society 95, 3941–3946.
- HIRAI T., SUZUKI K., KOMASAWA I., 2001, *Preparation and photocatalytic properties of composite CdS nanoparticles-titanium dioxide particles*, Journal of Colloid and Interface Science 244, 262–265.
- HUANG D.G., LIAO S.J., ZHOU W.B., QUAN S.Q., LIU L., HE Z.J., WAN J.B., 2009, *Synthesis of samarium- and nitrogen-co-doped TiO₂ by modified hydrothermal method and its photocatalytic performance for the degradation of 4-chlorophenol*, Journal of Physics and Chemistry of Solids 70, 853–859.
- IHARA T., MIYOSHI M., ANDO M., SUGIHARA S., IRIYAMA Y., 2001, *Preparation of a visible-light-active TiO₂ photocatalyst by RF plasma treatment*, Journal of Materials Science 36, 4201–4207.
- JCPDS International Center of Diffraction Data (1980), JCPDS Powder Diffraction File, Card 21-1272.
- LIU Y., CHEN X., LI J., BURDA C., 2005, *Photocatalytic degradation of azo dyes by nitrogen-doped TiO₂ nanocatalysts*, Chemosphere 61, 11–18.
- OHNO T., MITSUI T., MATSUMURA M., 2003, *Photocatalytic activity of S-doped TiO₂ photocatalyst under visible light*, Chemistry Letters 32, 364–365.
- TAKEUCHI K., NAKAMURA I., MATSUMOTO O., SUGIHARA S., ANDO M., IHARA T., 2000, *Preparation of visible-light-responsive titanium oxide photocatalysts by plasma treatment*, Chemistry Letters 29, 1354–1355.
- WANG J., MA T., ZHANG G., ZHANG Z., ZHANG X., JIANG Y., ZHAO G., ZHANG P., 2007, *Preparation of nanometer TiO₂ catalyst doped with upconversion luminescence agent and investigation on degradation of acid red B dye using visible light*, Catalysis Communications 8, 607–611.

- WANG J., TAFEN D.N., LEWIS J.P., HONG Z.L., MANIVANNAN A., ZHI M.J., LI M., WU N.Q., 2009, *Origin of photocatalytic activity of nitrogen-doped TiO₂ nanobelts*, Journal of the American Ceramic Society 131, 12290–12297.
- WEN L., LIU B., ZHAO X., NAKATA K., MURAKAMI T., FUJISHIMA A., 2012, *Synthesis, characterization, and photocatalysis of Fe-doped TiO₂: a combined experimental and theoretical study*, International Journal of Photoenergy, Article ID 368750, 10 pages, doi: 10.1155/2012/368750.
- WU X.H., QIN W., DING X.B., WEN Y., LIU H.L., JIANG Z.H., 2007, *Photocatalytic activity of Eu-doped TiO₂ ceramic films prepared by microplasma oxidation method*, Journal of Physics and Chemistry of Solids 68, 2387–2393.
- XU X.J., FANG X.S., ZHAI T.Y., ZENG H.B., LIU B.D., HU X.Y., BANDO Y., GOLBERG D., 2011, *Tube-in-tube TiO₂ nanotubes with porous walls: Fabrication, formation mechanism, and photocatalytic properties*, Small 7, 445–449.
- YAMASHITA H., HARADA M., MISAKA J., 2001, *Application of ion beam techniques for preparation of metal ion-implanted TiO₂ thin film photocatalyst available under visible light irradiation: Metal ion implantation and ionized cluster beam method*, Journal of Synchrotron Radiation 8, 569–571.
- YU J.C., ZHANG L., ZHENG Z., ZHAO J., 2003, *Synthesis and characterization of phosphated mesoporous titanium dioxide with high photocatalytic activity*, Chemistry of Materials 15, 2280–2286.
- ZHOU W., ZHENG Y., WU G., 2006, *Novel luminescent RE/TiO₂ (RE=Eu, Gd) catalysts prepared by in-situ sol-gel approach construction of multi-functional precursors and their photo or photocatalytic oxidation properties*, Applied Surface Science 252, 1387–1392.